Table 1. Changes in heart rate and blood pressure on day 0, before starting treatment, and on days 14 and 28 of pranidipine treatment in rats with heart failure after autoimmune myocarditis

	Heart rate, beats/min			SBP, mm Hg			MBP, mm Hg		
	day 0	day 14	day 28	day 0	day 14	day 28	day 0	day 14	day 28
Group N	350±11	346±8	362±14	114±3	112±7	114±4	97±2	96±3	99±3
Group V	352±10	349±7	358±12	95±3[a]	101±4	99±4	77±2[b]	78±3[a]	77±3[b]
Group 0.03	361±10	354±12	367±13	95±4[a]	90±5[a]	95±3[a]	73±3[b]	74±4[b]	77±3[b]
Group 0.3	357±14	342±10	352±7	94±4[a]	91±3[a]	91±3[b]	77±4[b]	69±2[b]	73±2[b]

Results are presented as the mean ± SE. SBP = Systolic blood pressure; MBP = mean blood pressure.

Group N, age-matched normal rats, received no treatment; group V, rats with heart failure treated with vehicle; group 0.03, rats with heart failure treated with low-dose pranidipine (0.03 mg/kg/day); group 0.3, rats with heart failure treated with high-dose pranidipine (0.3 mg/kg/day).

[a] $p < 0.05$, [b] $p < 0.01$ vs. group N.

Table 2. Changes in survival rate, histological, hemodynamic and echocardiographic parameters, and expression of TGF-β_1 and collagen-III mRNA in rats with heart failure after 4 weeks of treatment with pranidipine

	Group N (n = 10)	Group V (n = 10)	Group 0.03 (n = 8)	Group 0.3 (n = 10)
Survival rate, %	100	67[b]	73[b]	100**
Body weight, g	340±8	340±6	327±4	315±5
Heart weight, g	0.9±0.02	1.47±0.06[b]	1.33±0.05[b]	1.06±0.04**
H/B, g/kg	2.68±0.08	4.32±0.13[b]	4.07±0.16[b]	3.36±0.12**
Myocyte size, μm	10.4±0.04	16.3±0.25[b]	14.1±0.1[b]	11.6±0.1**
Area of fibrosis, %	3±1	36±2[b]	24±2[b]*	16±2[a]**
Heart rate, beats/min	320±7	307±11	274±9	288±8
Central venous pressure, mm Hg	−0.3±0.3	5.3±0.7[b]	4.9±1.2[b]	1.4±0.4*
Mean blood pressure, mm Hg	99±2	75±3[b]	71±5[b]	85±3
Left ventricular pressure, mm Hg	109±2	85±2[b]	82±5[b]	94±4
Left ventricular end-diastolic pressure, mm Hg	4±0.6	17±0.9[b]	12±1.7[b]	7±1.4*
+dP/dt, mm Hg/s	5,564±167	2,659±121[b]	2,838±215[b]	5,008±633
−dP/dt, mm Hg/s	−5,815±225	−2,516±141[b]	−3,213±307[b]	−4,891±608
Left ventricular diastolic dimension, mm	7.4±0.3	9.7±0.5[b]	nm	8.5±0.3[b]**
Left ventricular systolic dimension, mm	4.2±0.2	8.7±0.5[b]	nm	6.5±0.4[b]**
Fractional shortening, %	43±2	10±2[b]	nm	24±2[b]**
TGF-β_1, %	100	205±25[b]	151±17[a]	111±5*
Collagen-III, %	100	268±29[b]	231±38[a]	91±15**

Results are presented as the mean ± SE.

Group N, age-matched normal rats, received no treatment; group V, rats with heart failure treated with vehicle; group 0.03, rats with heart failure treated with low-dose pranidipine (0.03 mg/kg/day); group 0.3, rats with heart failure treated with high-dose pranidipine (0.3 mg/kg/day).

[a] $p < 0.05$, [b] $p < 0.01$ vs. group N; * $p < 0.05$, ** $p < 0.01$ vs. group V. nm = Not measured.

Myocyte diameter measurements were performed in 10 myocytes selected per field in 400-fold magnification by the use of light microscopy. Short axis diameters of each myocyte were measured from hearts of different groups. Each average value was obtained based on the data from 10 myocytes and was used as an independent sampling data.

Ribonuclease Protection Assay

The apical left ventricle from each of the four groups was quickly excised, frozen in liquid nitrogen, and stored at −80°C. The total RNA was extracted from the tissues by the acid guanidium-isothiocyanate-phenol-chloroform method [26]. Antisense complementary RNA probes for transforming growth factor-β_1 (TGF-β_1), collagen-III

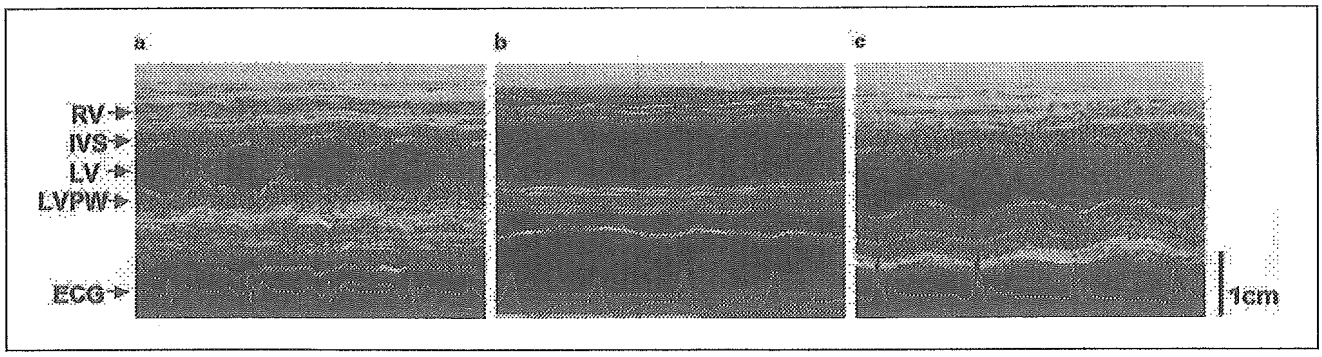

Fig. 1. Representative M-mode echocardiograms obtained after 4 weeks of pranidipine treatment in rats with heart failure. **a** Group N, **b** group V, **c** group 0.3.

and glyceraldehyde-3-phosphate dehydrogenase (GAPDH) were generated as described previously [27]. The ribonuclease protection assays for the quantification of TGF-β_1, collagen-III mRNA levels was performed as described previously [27]. The results for each mRNA were normalized to those for GAPDH mRNA in each sample.

Statistical Analysis

Data are presented as mean ± SEM. Statistical analysis between the groups was performed by one-way ANOVA, followed by Tukey's method. Differences were considered to be significant at $p < 0.05$.

Results

Changes in Heart Rate, SBP and MBP after Oral Administration of Pranidipine during the Course of Treatment in Rats with Heart Failure

Changes in heart rate, SBP and MBP are shown in table 1. The heart rate did not change during the course of treatment. On day 0, no differences in SBP and MBP were observed between the pranidipine- and vehicle-treated rats. Although pranidipine decreased SBP and MBP in rats with heart failure, there were no significant differences between group 0.03 and group 0.3 compared with group V on days 14 and 28.

Clinical Course

Five (33%) of 15 rats and 3 (27%) of 11 rats in group V and group 0.03 died between days 28 and 56, respectively (table 2). All hearts from dead rats showed extensive myocardial fibrosis and massive pericardial effusion. None of the rats died in group 0.3 and group N. The 56-day survival rate was significantly higher in group 0.3 than in group V ($p < 0.01$).

Body Weight and Heart Weights

Body weight, HW and H/B are summarized in table 2. The body weight did not differ among the three groups with heart failure. HW and H/B were significantly greater in group V than in group N. Pranidipine reduced the HW and H/B in a dose-dependent manner, and the effects were significant in group 0.3 compared with group V.

Hemodynamic Parameters

The hemodynamic parameters are shown in table 2. The heart rate did not differ among the four groups. CVP and LVEDP were significantly higher and MBP, peak LVP and ± dP/dt were significantly lower in group V than those in group N. Pranidipine treatment reduced CVP and LVEDP in a dose-dependent manner, and the effect was significant only in group 0.3. Although pranidipine greatly increased the ± dP/dt in group 0.3, its effects on MBP and LVP were not significant compared to group V.

Echocardiographic Measurements

The results of echocardiography are presented in figure 1 and table 2. LVDd and LVDs were higher, and FS and EF were lower in group V than those in group N. Compared with group V, pranidipine treatment resulted in a significant decrease in both LVDd and LVDs in group 0.3. Consequently, FS were significantly increased in group 0.3 compared to those in group V.

Myocardial Fibrosis and Cell Size

Figure 2 shows representative photographs of thin sections of heart stained with the Azan-Mallory method. The hearts in group V showed massive fibrosis compared to group N. Pranidipine treatment significantly attenuated

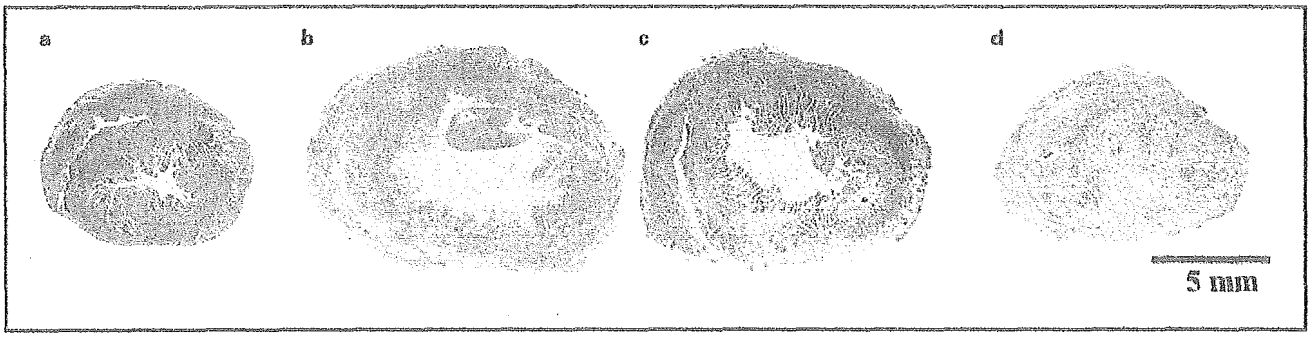

Fig. 2. Myocardial fibrosis and the effects of pranidipine after 4 weeks of treatment in rats with heart failure. A representative photograph of each group stained with Azan-Mallory is shown in which the blue area indicates fibrosis as opposed to the red myocardium. **a** Group N, **b** group V, **c** group 0.03, **d** group 0.3.

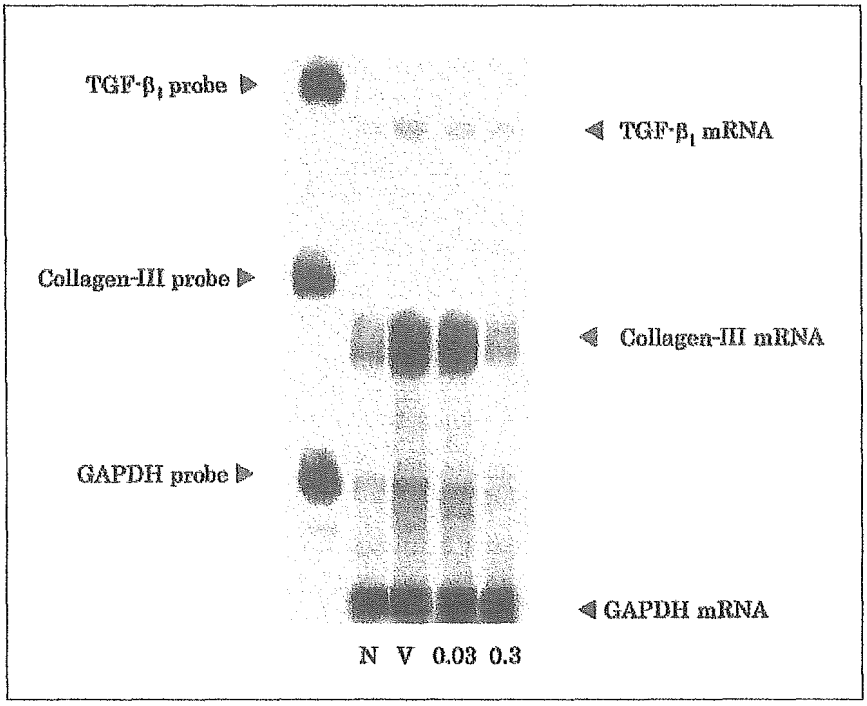

Fig. 3. Effects of pranidipine on the mRNA expression of TGF-β_1 and collagen-III in rats with heart failure. Oral administration of pranidipine for 1 month reduced the expression TGF-β_1 and collagen-III mRNA in the left ventricle. N, age-matched normal rats; V, rats with heart failure; 0.03 and 0.3 treatment with 0.03 and 0.3 mg/kg/day of pranidipine respectively. GAPDH, glyceraldehyde-3-phosphatedehydrogenase.

the area of fibrosis in both group 0.03 and group 0.3 compared with group V. The myocyte size in group V was significantly larger than that in group N, and the pranidipine treatment significantly reduced the increase in myocyte size in group 0.3. However, the pranidipine treatment did not provide any significant changes in myocyte size in group 0.03 (table 2).

Expression of TGF-β_1 and Collagen-III mRNA in the Left Ventricle

As shown in figure 3, the levels of left ventricular mRNA expression of TGF-β_1 and collagen-III were markedly increased in group V as compared with group N. Pranidipine treatment significantly reduced expression of TGF-β_1 and collagen-III in group 0.3, but not in group 0.03 than in group V (table 2).

Discussion

In this study, we examined the effects of chronic treatment with pranidipine on the development of myocardial dysfunction and remodeling in rats with heart failure immunized by porcine cardiac myosin. Our results demonstrated that treatment with pranidipine prevented progressive left ventricular dysfunction and remodeling in rats with heart failure. High-dose pranidipine (group 0.3) significantly improved the survival rate and ±dP/dt, reduced HW, H/B, area of fibrosis and decreased CVP, LVEDP more effectively than low-dose pranidipine (group 0.03) compared to group V. It was also found to reduce the myocardial mRNA expression of TGF-β_1 and collagen-III in a dose-dependent manner.

Calcium channel antagonists are clinically effective vasodilators, and are widely used for the treatment of hypertension and angina pectoris. However, the effectiveness of calcium channel antagonists in the treatment of patients with heart failure is controversial [28]. From the pharmacological point of view, there are three major categories of calcium channel antagonists: dihydropyridines, phenylalkylamines, and benzothiazepines among which the dihydropyridines possess greater vasodilator selectivity compared to negative inotropic action [29]. Dihydropyridine calcium antagonists have a wide range of antioxidant potencies and may indeed protect myocardial membrane phospholipid from peroxidative injury [30]. Some dihydropyridines are reported to inhibit NO production and proinflammatory cytokines [31–33]. Pranidipine is a third-generation calcium channel antagonist in the dihydropyridine class, with potent antihypertensive activity [18, 19], devoid of a negative inotropic effect, and has direct venodilatory action [20]. Pranidipine upregulates the activity of superoxide dismutase, a superoxide scavenger, and thus inhibits NO decomposition in vascular wall [34]. These actions of pranidipine might be some beneficial features for its therapeutic indication in heart failure.

Cardiac myosin-induced autoimmune myocarditis, which was not exclusively related to viral infection, was demonstrated to progress into the clinicopathological state, similar to dilated cardiomyopathy in the chronic phase, and was characterized by the enlargement of the heart, dilatation of both ventricles, diffuse and extensive myocardial fibrosis, and hypertrophic and atropic changes of myocardial fibers resembled human cardiomyopathy [7–9]. In this model of heart failure, pranidipine exerted beneficial hemodynamic effects in a dose-dependent manner. It significantly reduced CVP and LVEDP without changing the heart rate. In the failing heart, abnormal intracellular calcium handling may lead to cardiac dysfunction associated with a variety of structural and biochemical abnormalities [35–37]. Pranidipine, in addition to its beneficial hemodynamic effects, may prevent calcium overload by reducing trans-sarcolemmal calcium conductivity, particularly through L-type voltage-dependent calcium channels, and thereby stabilize cellular calcium homeostasis and maintain intact function and structural integrity of hearts in rats with heart failure.

The expression of mRNA for TGF-β_1, a multifactorial cytokine that plays a major role in the regulation of extracellular matrix deposition [38], and the increased interstitial collagen level in myocardium may enhance organ stiffness and results in cardiac dysfunction, eventually leading to heart failure [39]. Pranidipine is reported to prevent the development of ventricular remodeling and reduced collagen levels after myocardial infarction in rats [23]. In this study, pranidipine reduced the left ventricular mRNA expression of TGF-β_1, collagen-III and attenuated myocardial fibrosis. High-dose pranidipine prevented progression of left ventricular systolic and diastolic dysfunction as evidenced by the improvement of FS and ±dP/dt compared with group V. Furthermore, high-dose pranidipine reduced myocyte size, HW, LVDd and LVDs, and was suggestive of regression of myocardial hypertrophy, cavity dilatation and stiffness. These results may account for the beneficial effects of pranidipine on heart failure and propose a new effect of this drug on suppression of TGF-β_1.

Conclusion

The present study indicates that pranidipine increases survival rate, prevents systolic and diastolic dysfunction, and attenuates myocardial fibrosis and left ventricular remodeling in rats with heart failure after autoimmune myocarditis, and that the cardioprotective effects of pranidipine may be partially explained by suppression of the fibrotic response through the inhibition of TGF-β_1 and collagen-III mRNA expression and regression of myocyte hypertrophy. However, the mechanism by which pranidipine attenuates fibrotic response and expression of TGF-β_1 in our model of heart failure remains to be elucidated.

Acknowledgements

This research was supported by the grants from the Yujin Memorial Grant, Ministry of Education, Science, Sports and Culture of Japan and the Promotion and Mutual Aid Corporation for Private Schools of Japan.

References

1 Taliercio CP, Seward JB, Driscoll DJ, Fisher LD, Gersh BJ, Tajik AJ: Idiopathic dilated cardiomyopathy in the young: Clinical profile and natural history. J Am Coll Cardiol 1985;6: 1126–1131.

2 Roberts WC, Siegel RJ, McManus BM: Idiopathic dilated cardiomyopathy: Analysis of 152 necropsy patients. Am J Cardiol 1987;60: 1340–1355.

3 Dec GW, Palacios IF, Fallon JT, Aretz HT, Mills J, Lee DCS, Johnson RA: Acute myocarditis in the spectrum of acute dilated cardiomyopathies: Clinical features, histologic correlates, and clinical outcome. N Engl J Med 1985; 312:885–890.

4 Matsumori A, Kawai C: An animal model of congestive (dilated) cardiomyopathy: Dilatation and hypertrophy of the heart in the chronic stage in DBA/2 mice with myocarditis caused by encephalomyocarditis virus. Circulation 1982;66:355–360.

5 Klingel K, Hohnenadl C, Canu A, Albrecht M, Seeman M, Mall G, Kandolf R: Ongoing enterovirus-induced myocarditis is associated with persistent heart muscle infection: Quantitative analysis of virus replication, tissue damage and inflammation. Proc Natl Acad Sci USA 1992; 89:314–318.

6 Davidoff R, Palacios I, Southern J, Fallon JT, Newell J, Dec GW: Giant cell versus lymphocytic myocarditis: A comparison of their clinical features and long-term outcomes. Circulation 1991;83:953–961.

7 Kodama M, Matsumoto Y, Fujiwara Y, Masani F, Izumi T, Shibata A: A novel experimental model of giant cell myocarditis induced in rats by immunization with cardiac myosin fraction. Clin Immunol Immunopathol 1990; 57:250–262.

8 Kodama M, Hanawa H, Saeki M, Hosono H, Inomata T, Suzuki K, Shibata A: Rat dilated cardiomyopathy after autoimmune giant cell myocarditis. Circ Res 1994;75:278–284.

9 Watanabe K, Ohta Y, Nakazawa M, Higuchi H, Hasegawa G, Naito M, Fuse K, Ito M, Hirono S, Tanabe N, Hanawa H, Kato K, Kodama M, Aizawa Y: Lowdose carvedilol inhibits progression of heart failure in rats with dilated cardiomyopathy. Br J Pharmacol 2000; 130:1489–1495.

10 Kloner RA, Przyklenk K: Progress in cardioprotection: The role of calcium antagonists. Am J Cardiol 1990;66:H2–H9.

11 Triggle DJ: Calcium antagonists; in Antonaccio M (ed): Cardiovascular Pharmacology. New York, Raven Press, 1990, pp 107–160.

12 Kloner RA, Braunwald E: Effects of calcium antagonists on infarcting myocardium. Am J Cardiol 1987;59:B84–B98.

13 Tatani A, Kunze DI, Brown AM: Effects of dihydropyridine calcium channel modulators on cardiac sodium channels. Am J Physiol 1988;254:H140–H147.

14 Henry PD: Antiperoxidative actions of calcium antagonists and atherogenesis. J Cardiovasc Pharmacol 1991;18(suppl 1):6–10.

15 Elkayam U, Amin J, Mehra A, Vasquez J, Weber L, Rahimtoola SH: A prospective, randomized, double-blind, crossover study to compare the efficacy and safety of chronic nifedipine therapy with that of isosorbide dinitrate and their combination in the treatment of chronic congestive heart failure. Circulation 1990;82:1954–1961.

16 Barjon JN, Rouleau JL, Bichet D, Juneau C, De Champlain J: Chronic renal and neurohumoral effects of the calcium entry blocker nisoldipine in patients with congestive heart failure. J Am Coll Cardiol 1987;9:622–630.

17 Goldstein RE, Boccuzzi SJ, Cruess D, Nattel S: Adverse Experience Committee, Multicenter Diltiazem Postinfarction Research Group. Diltiazem increases late-onset congestive heart failure in postinfarction patients with early reduction in ejection fraction. Circulation 1991; 83:52–60.

18 Nakayama N, Ikezono K, Mori T, Yamashita S, Nakayama S, Tanaka Y, Hosokawa T, Minami Y, Masutani K, Yamamura Y, Yabuuchi Y: Antihypertensive activity of OPC-13340, a new potent and long-acting dihydropyridine calcium antagonist, in rats. J Cardiovasc Pharmacol 1990;15:836–844.

19 Mori T, Nakayama N, Ohura M, Ikezeno K, Kinoshita S, Kamata M, Hosokawa T, Yamashita S, Yabuuchi Y: Cardiovascular effects of OPC-13340, a potent, long-acting 1,4-dihydropyridine calcium channel blocker, in dogs. Arch Int Pharmacodyn Ther 1993;321:41–56.

20 Hirano T, Ohura M, Orito K, Fujiki H, Miyakoda G, Mori T: Venodilator effects of pranidipine, a 1,4-dihydropyridine Ca^{2+} channel antagonist, in rats: Comparison with nifedipine and amlodipine. Eur J Pharmacol 1997;324: 201–204.

21 Nakayama N, Ikezono K, Ohura M, Yabuuchi Y: Effect of the new long-acting dihydropyridine calcium antagonist pranidipine on the endothelium-dependent relaxation in isolated rat aorta in vitro. Arzneimittelforschung 1993;43: 1266–1270.

22 Mori T, Takeuchi T, Ohura M, Miyakoda G, Fujiki H, Orito K, Yoshida K, Hirano T, Yamamura Y, Sumida T, Nakaya Y, Sarake H, Hata F: Pranidipine, a new 1,4-dihydropyridine calcium channel blocker, enhances cyclic GMP-independent nitric oxide-induced relaxation of the rat aorta. Mol Cell Biochem 1998; 178:335–343.

23 Takeuchi K, Omura T, Yoshiyama M, Yoshida K, Otsuka R, Shimada Y, Ujino K, Yoshikawa J: Long-acting calcium channel antagonists pranidipine prevents ventricular remodeling after myocardial infarction in rats. Heart Vessels 1999;14:111–119.

24 Kim CS, Matsumori A, Goldberg L, Doye AA, McCoy Q, Gwathmey JK: Effects of pranidipine, a calcium channel antagonist, in an avian model of heart failure. Cardiovasc Drugs Ther 1999;13:455–463.

25 Uehara Y, Kawabata Y, Ohshima N, Hirawa N, Takada S, Numabe A, Nagata T, Goto A, Yagi S, Omata M: New dihydropyridine calcium channel antagonist, pranidipine, attenuates hypertensive renal injury in Dahl salt-sensitive rats. J Cardiovasc Pharmacol 1994;23: 970–979.

26 Chomczynski P, Sacchi N: Single-step method of RNA isolation by acid guanidium-isothiocyanate-phenol-chloroform extraction. Anal Biochem 1987;162:156–159.

27 Ohta Y, Watanabe K, Nakazawa M, Yamamoto T, Ma M, Fuse K, Ito M, Hirono S, Tanabe N, Hanawa H, Kato K, Kodama M, Aizawa Y: Carvedilol enhances atrial and brain natriuretic peptide mRNA expression and release in rat heart. J Cardiovasc Pharmacol 2000;36(suppl 2):19–23.

28 Packer M, Kessler PD, Lee WH: Calcium channel blockade in the management of severe chronic congestive heart failure: A bridge too far. Circulation 1987;75(suppl V): 56–64.

29 Taira N: Differences in cardiovascular profile among calcium antagonists. Am J Cardiol 1987;59:B24–B29.

30 Janero DR, Burghardt B: Antiperoxidative effects of dihydropyridine calcium antagonists. Biochem Pharmacol 1999;38:4344–4348.

31 Szabo C, Thiemermann C, Vane JP: Dihydropyridine antagonists and agonists of calcium channels inhibit the induction of nitric oxide synthase by endotoxin in cultured macrophages. Biochem Biophys Res Commun 1993; 196:825–830.

32 Mahe Y, Wakasugi H, Scamps C, Chousaib S, Tursz T: Role of calcium on interleukin-1 production by monocytes: Its relevance during T-cell proliferation. Lymphokine Cytokine Res 1991;10:165–172.

33 Yuan Z, Kishimoto C, Shioji K: Beneficial effects of benedipine in acute autoimmune myocarditis: Suppressive effects on inflammatory cytokines and inducible nitric oxide synthase. Circ J 2003;67:545–550.

34 Yang J, Fukuo K, Morimoto S, Niinobu T, Suhara T, Ogihara T: Pranidipine enhances the action of nitric oxide released from endothelial cells. Hypertension 2000;35:82–85.

35 Katz AM: Cardiomyopathy of overload: A major determinant of prognosis in congestive heart failure. N Engl J Med 1990;322:100–110.

36 Morgan JP, Erny RE, Allen PD, Grossman W, Gwathmey JK: Abnormal intracellular calcium handling, a major cause of systolic and diastolic dysfunction in ventricular myocardium from patients with heart failure. Circulation 1990; 81(suppl III):21–32.

37 Bristow MR, Hershberger RE, Port DJ, Gilbert EM, Sandoval A, Rasmussen R, Cates AE, Feldman AM: β-Adrenergic pathways in nonfailing and failing human ventricular myocardium. Circulation 1990;82(suppl I):12–25.

38 Boluyt MO, O'Neill L, Meredith AL, et al: Alterations in cardiac gene expression during the genes encoding extracellular matrix components. Circ Res 1994;75:22–32.

39 Weber KT, Sun Y, Tyagi SC, Cleutjens JP: Collagen network of the myocardium: function, structural remodeling and regulatory mechanisms. J Mol Cell Cardiol 1994;26:279.

Available online at www.sciencedirect.com
SCIENCE DIRECT®

Gene 332 (2004) 179–190

GENE
AN INTERNATIONAL JOURNAL ON GENES AND GENOMES

www.elsevier.com/locate/gene

Comparative analysis of gene expression mechanisms between group IA and IB phospholipase A_2 genes from sea snake *Laticauda semifasciata*☆

Takahiko J. Fujimi, Sakiko Yasuoka, Eri Ogura, Takahide Tsuchiya, Toru Tamiya*

Department of Chemistry, Faculty of Science and Technology, Sophia University, 7-1, Kioi-cho, Chiyoda-ku, Tokyo 102-8554, Japan

Received 2 October 2003; received in revised form 10 February 2004; accepted 27 February 2004

Received by Takashi Gojobori

Available online 17 April 2004

Abstract

Phospholipase A_2 (PLA_2) genes expressed in the venom glands of the sea snake, *Laticauda semifasciata*, were investigated. Both mRNAs, encoding group IA (without a pancreatic loop) and group IB (with pancreatic loop), were detected from venom glands by Northern blot hybridization analysis and RT-PCR. The results of quantitative PCR analysis indicated that the expression amount of group IA genes was around 100–300 times greater than that of group IB genes. Sequence analysis of 5′-upstream regions and a reporter gene assay of the genes (groups IA and IB) previously cloned showed that the functional sequence (411 bp) was inserted in the 5′-flanking region of the group IA PLA_2 genes. It seemed that the contribution of the inserted sequence to the amount of transcribed mRNAs was greater than that of number of genes present in the genome. Comparative analysis of the 5′-flanking sequences from several snake genes encoding toxic PLA_2s revealed that this sequence was probably inserted into an ancestral gene of PLA_2 with a pancreatic loop. After the duplication of the gene, which contained the inserted sequence, the PLA_2 gene without a pancreatic loop evolved from one of the duplicate genes. This inserted sequence might determine the future of the genes expressed in the venom glands.

Keywords: Snake toxin; Phospholipase A_2; Molecular evolution; Promoter

1. Introduction

Phospholipase A_2 (PLA_2, EC 3.1.1.4) catalyzes the hydrolysis of the acyl ester bond at the *sn*-2 position of phosphoglycerides (Tischfield, 1997). Phospholipase A_2s are commonly classified into twelve groups and many subgroups (Six and Dennis, 2000). Snake venoms are well known as good sources of low molecular weight secreted type PLA_2s. Venoms of the Viperidae and Colubridae families contain group II PLA_2s, whereas venoms of the Elapidae family contain group I PLA_2s. Phospholipase A_2s in group I are further divided into two subgroups, IA and IB. The difference between these two subgroups is the existence (IB) or the absence (IA) of a pancreatic loop in their amino acid sequences. The digestive PLA_2s secreted as zymogens in the pancreas of mammals are classified into group IB PLA_2. In mammals, group IB PLA_2 is well known as an enzyme contributed to the some pharmacological responses in the cells mediated through the arachidonic acid releasing or the specific receptor binding (Tohkin et al., 1993; Fonteh et al., 1998; Yokota et al., 2000).

Most of toxic PLA_2s from the venoms of the Elapidae family are classified into group IA PLA_2s (*Naja*, Bhat et al., 1991; *Notechis*, Halpert and Eaker, 1976; *Laticauda*, Yoshida et al., 1979). Snake venomous PLA_2s with a pancreatic loop (IB) have been isolated from the venom of *Oxyuranus*

Abbreviations: GADPH, glyceraldehyde-3-phosphate dehydrogenase; GL, genomic library; LsGADPH, *Laticauda semifasciata* glyceraldehyde-3-phosphate dehydrogenase; LsPLA2, *Laticauda semifasciata* phospholipase A_2; PCR, polymerase chain reaction; RT-PCR, reverse transcription-polymerase chain reaction.

☆ The nucleotide sequence data reported here have been submitted to the DDBJ sequence data bank. The 5′-upstream regions of group IA and IB PLA_2 genes from *L. semifasciata*, IA: AB111958, IB: AB111959; Group IB PLA_2 mRNA partial sequences from *L. semifasciata* venom glands, AB120375 (VG11) and AB120376 (VG8); GAPDH mRNA partial sequence from, *L. semifasciata* AB111960.

* Corresponding author. Tel.: +81-3-3238-3363; fax: +81-3-3238-3361.

E-mail address: t_tamiya@sophia.ac.jp (T. Tamiya).

0378-1119/$ - see front matter © 2004 Elsevier B.V. All rights reserved.
doi:10.1016/j.gene.2004.02.050

scutellatus scutellatus (Fohlman et al., 1976; Lambeau et al., 1990), *Pseudonaja textilis* (Pearson et al., 1991), *Micropechis ikaheka* (Gao et al., 1999) and *Notechis scutatus scutatus* (Francis et al., 1995). Both types of PLA_2s (groups IA and IB) have been purified as one of the toxic components from the venoms of the snake species, mentioned above, *P. textilis*, *O. scutellatus scutellatus* and *N. scutatus scutatus* (Danse et al., 1997).

Although toxin genes expressed in the snake venom glands, almost nothing is known about the mechanism of the expression regulation system. Jeyaseelan et al. (2000, 2001) and Ma et al. (2001) assessed the promoter activity of several snake toxin genes, including the group IA PLA_2 gene, using a reporter gene assay. They have found that the promoter activities of the snake toxin genes in the CHO cells are proportional to their in vivo expression levels (Jeyaseelan et al., 2001; Ma et al., 2001).

We have reported the nucleotide sequences of genes encoding groups IA and IB PLA_2s from the genomic library and cDNAs cloned from the venom gland (IA) and pancreas (IB) cDNA pools of *Laticauda semifasciata* (Table 1) (Fujimi et al., 2002a,b). Analyses of the structural genes of both group IA and IB PLA_2 revealed that they evolved from the same ancestral gene, and the expression products acquired the character of digestive enzymes or toxins. However, the regulation mechanisms of transcription involved in the diversification of these PLA_2 genes were still not understood. It is very important to clarify the regulation mechanisms of transcription in the venom glands, because the gene expression in the appropriate tissue is necessary for the expression product to act as a toxin.

In this report, the expression of group IB PLA_2 genes in the venom gland of *L. semifasciata* was proven by Northern blot hybridization and RT-PCR. The result of Northern blot hybridization and quantitative PCR analyses also showed that the expression levels of group IB genes in venom glands were quite low compared with those of the group IA genes. To elucidate the cause of the vast difference about the expression levels of both groups of genes, a series of reporter gene assay and gene quantitative analysis were performed. The reporter gene assay of group IA and IB genes from *L. semifasciata* using CHO-K1 cells, showed that the specific sequence was present in the promoter regions of the group IA gene and suggested the group IA specific sequence played an important role in the gene expression.

Table 1
Description regarding *L. semifasciata* phospholipase A_2 clones used in this study

Clone name	Accession no.	Clone type	Group	Origin
LsPLA2cPm09	AB037415	cDNA	IA	venom gland
LsPLA2pkP5	AB078348	cDNA	IB	pancreas
VG11[a]	AB120375	cDNA	IB	venom gland
VG8[a]	AB120376	cDNA	IB	venom gland
LsPLA2GL1-1	AB062439	gene	IA	genom library
LsPLA2GL5-1	AB062440	gene	IA	genom library
LsPLA2GL16-1	AB078346	gene	IB	genom library
1-1up1[a]	AB111958	upst ream of LsPLA2GL1-1	–	genom library
16-1up1[a]	AB111959	upstream of LsPLA2GL16-1	–	genom library

[a] These clones were newly reported in this report. The other clones had been reported in our previous reports (Fujimi et al., 2002a,b).

2. Materials and methods

2.1. Synthesis of single-stranded cDNA pool

Total RNA was extracted from 1 g of frozen venom glands using TRIZOL, according to the manufacturer's protocol (Invitrogen). Poly(A)$^+$ RNA was purified from total RNA with Dynabeads Oligo $(dT)_{25}$ (Dynal). Single-stranded cDNA (cDNA pool) was synthesized by reverse transcriptase M-MLV (Takara) with an anchored oligo (dT) primer (5′-CTGATCTAGAGGTACCGGATCCT$_{20}$-3′) according to the manufacturer's protocol.

2.2. PCR amplification, cloning and sequence determination of PLA_2 cDNAs

Three primers were used (#3AB: 5′-CATYKWGCTTGCAGITTCACCAC-3′, #4AB: 5′-ATYGGCACCTCACTTTATTGTTCA-3′ and loopF: 5′-ACATCCTGCATGTAAGTCCC-3′) for amplification of PLA_2 cDNAs from the cDNA pool (Fig. 1). The primers #3AB and #4AB were designed to anneal with cDNAs that encoded both groups of PLA_2s (IA and IB). The sequence of loop F primer is complimentary to the pancreatic loop coding sequence of LsPLA2pkP5 (DDBJ accession number AB078348). Amplified fragments were cloned using pGEM-T Easy vector systems (Promega) and plasmid DNAs obtained were purified by Wizard plus Minipreps DNA Purification Systems (Promega).

2.3. Probes for hybridization analysis

Partial sequences of cDNA clones LsPLA2cPm09 (group IA PLA_2: AB037415) from venom glands and LsPLA2pkP5 (group IB PLA_2: AB078348) from the pancreas (Fujimi et al., 2002a,b) were amplified by PCR using IBF (5′-ACAGGCATCGCCCACCCACCTG-3′), IBR (5′-ATTGCACTCAGCCCCGTTTG-3′), IAF (5′-TAGGTGCTCCAAAATACATG-3′) and #8EP (5′-TTGAATTCTGCAGAGGCCCATCCAGAGAATTGCCAT-3′) as primers. Origins and accession numbers of the template cDNA clones are described in Table 1. The positions and directions of the primers are indicated in Fig. 1A. A cDNA clone encoding the partial sequence of *L. semifasciata* glyceraldehyde 3-phosphate dehydrogenase (LsGAPDH: AB111960), previously cloned, was used for the probe for detection of LsGAPDH mRNA. The fragments obtained were then purified by agarose gel electrophoresis and labeled by the ECL direct nucleic acid

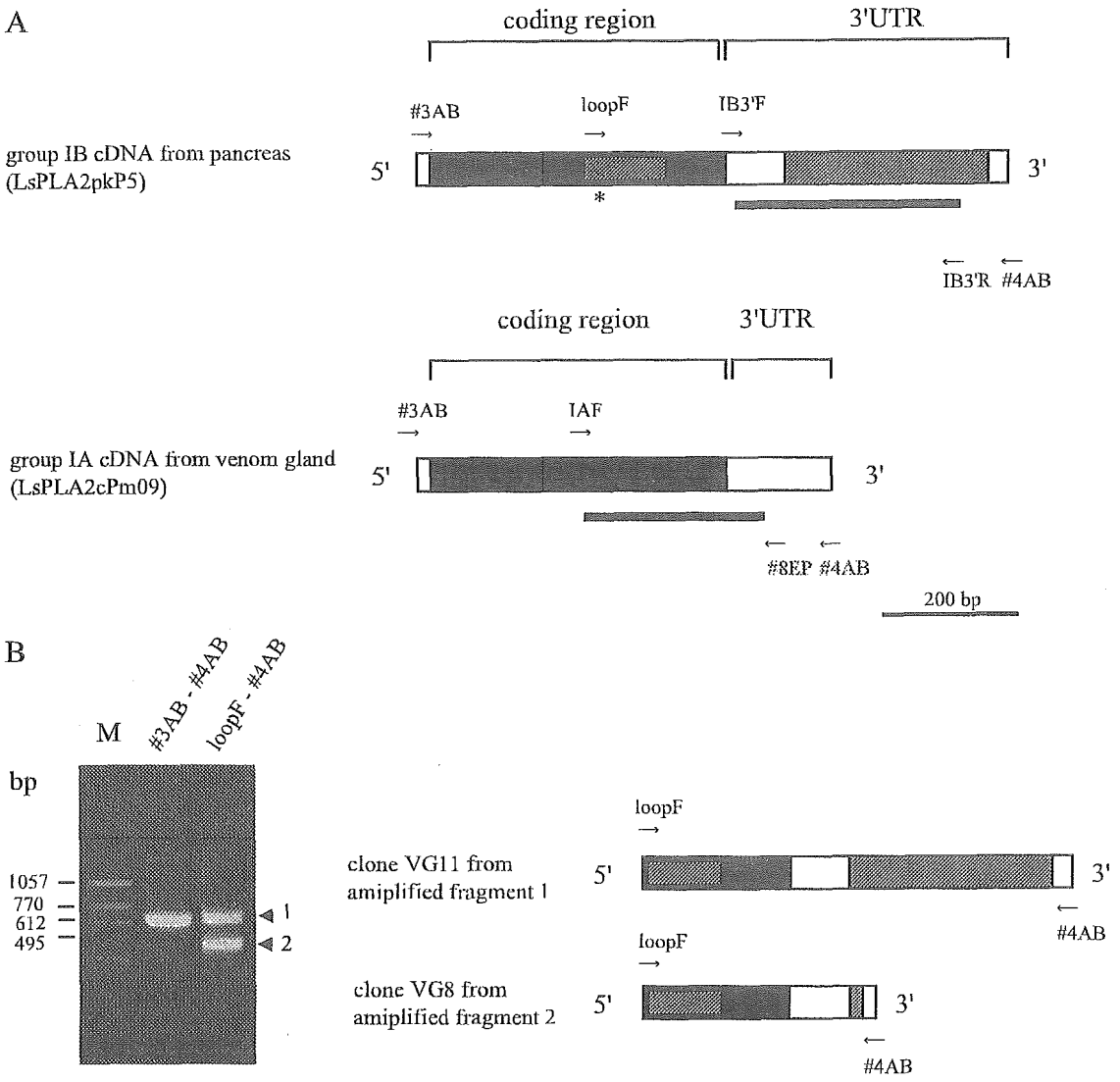

C

```
pkP5        -27   MNPAHLLVLLAVCVSLLGASTIPPLPLNLVQFSNMIKCTIPGSRPLLDYADYGCYCGAGG  33

pkP5         34   SGTPVDELDRCCQTHDNCYSQAKKHPACKSPLDSPYIKIYSYTCSGGSLTCRDDNDECGA  93
VG11                                    LDSPYIKIYSYTCSGGSLTCRDDNDECGA
VG8                                     LDSPYIKIYSYTCSGGSLTCRDDNDECGA

pkP5         94   FICNCDRTAAICFAGAPYNKENYNIDTKKHCK  125
VG11              FICNCDRTAAICFAGAPYNKENYNIDTKKHCK
VG8               FICNCDRTAAICFAGAPYNKENYNIDTKKHCK
```

Fig. 1. Cloning of group IA and IB PLA_2 cDNAs from venom glands. (A) Schematic comparison of typical cDNA clones encoding group IA (LsPLA2cPm09) and IB (LsPLA2pkP5) PLA_2s. Arrows indicate the annealing positions and directions of the primers. The regions with black or white color are highly homologous to each other. The regions in gray indicate the low homology between the two groups. An asterisk shows the position of the pancreatic loop coding sequence. Bold underlines indicate the annealing region of probes for Northern blot hybridization analysis. (B) Amplification of partial group IB PLA_2 cDNA from the cDNA pool of venom glands by PCR. Left: Agarose gel (2%) electrophoresis of amplified fragments. M indicates the DNA size marker. The primers used for amplification are represented above the each lane. Arrow heads with numbers (1 and 2) in the right side of the bands indicate the two amplified fragments of different sizes obtained by PCR using loop F and #4AB as primers. Schematic drawings of the clones from each amplified fragment (VG8 and VG11) are indicated on the right. (C) Comparisons of partial amino acid sequences of VG8, VG 11 and pancreas group IB PLA_2 deduced from the clone LsPLA2pkP5 (pkP5).

labeling and detection system (Amersham Pharmacia Biotech) according to the manufacturer's protocol. Specificity of the probes was checked by Southern blot hybridization analysis using the same detection system as Northern blot analysis.

2.4. Northern blot hybridization analysis

Poly(A)$^+$ RNAs purified from the 100 μg total RNAs (venom glands or pancreas) by Dynabeads Oligo $(dT)_{25}$ (Dynal), and electrophoresed on a 1% formaldehyde agarose gel. RNAs in the agarose gel were transferred on Hybond-N+ (Amersham Pharmacia Biotech) by aspiration, and then fixed by UV. Phospholipase A_2 mRNAs on the blotted membrane were detected by the ECL direct nucleic acid labeling and detection system (Amersham Pharmacia Biotech) and X-ray film (X-OMAT AR film, KODAK) according to the manufacturer's protocols. Exposure time was an important factor to detect the probe specific signal, especially when the quantity of target mRNAs was low, because the intensity of the detected bands on the X-ray film was the integrated value of chemiluminescence. To obtain the sufficient or moderate signals, three X-ray films were exposed with time variance (10 min, 2 h and 12 h) per an assay using a probe. The same membrane was reacted sequentially with three kinds of probes to detect mRNA encoding GAPDH, group IB PLA_2 and group IA PLA_2.

2.5. Cloning and sequence analysis of 5′-upstream regions of PLA_2 genes

Lambda FIXII (Stratagene) genomic clones, LsPLA-2GL1-1 (group IA) and LsPLA2GL16-1 (group IB) were digested with *Hin*dIII (for group IA), and *Cla*I and *Bam*HI (for group IB). The DNA fragments corresponding to −3742 to +1571 of LsPLA2GL1-1, and −6514 to +129 of LsPLA2GL16-1 were inserted into pBluescript II SK(+) vectors (Stratagene). The subclones obtained were named 1-1up1 (group IA) and 16-1up1 (group IB). Origins and accession numbers of the clones are summarized in Table 1.

2.6. Construction of the vectors for reporter gene assay

The 5′-upstream region containing the conserved sequence for the gene of each group (IA and IB) was amplified by PCR using 1-1up1 as a template and the following primers: F2AMlu (5′-ACGCGTAAATGAGAG-CAGATTTCCGT-3′) and RAXho (5′-CTCGAGTTTGT-CAGTGGTGAAGCTGC-3′). The amplified fragment was digested with *Mlu*I and *Xho*I, and ligated into the pGL3-Basic vector (Promega). A Kilo-Sequence deletion Kit (Takara) was used to generate the 5′-progressive deletion mutant series of the 5′-upstream region of the group IA PLA_2 gene. Clones containing a suitable length of the 5′-upstream region were selected and sequenced. Finally, the reporter gene series of the group IA PLA_2 gene 5′-upstream region (IA-633, -545, -410, -382, -232, -162, -83 and -33) was obtained. For the group IB PLA_2 gene 5′-upstream region, three sense primers [for IB-220: F2Bmlu (5′-ACGCGTAAATCAGAGCAGATTTCCGT-3′), for IB-220: F150Mlu (5′-ACGCGTACAGCTCTGGTTTTATCTCC-3′) and for IB-33: F33Mlu (5′-ACGCGTGCTATAAAAGGTT-GAACTCG-3′)] and one antisense primer [RBXho (5′-CTCGAGTTTGTCTGTGGTGAATCTGC-3′)] were used for amplification of appropriate regions. The amplified fragments were digested with *Mlu*I and *Xho*I, and ligated into the pGL3-Basic vector (Promega). Finally, the reporter gene series of the group IB PLA_2 gene 5′-upstream region (IB-220, -132 and -33) was obtained.

2.7. Cell culture and DNA transfection

The Chinese hamster ovary cell K1 line (CHO-K1) was used for a luciferase assay of *L. semifasciata* PLA_2 genes. The cell line was maintained in an α-MEM medium supplement with 10% fetal bovine serum. The day before transfection, cells were trypsinized and subcultured into a 24-well plate at a density of 5.0×10^4 cells per well. To normalize for transcriptional efficiency, a pRL-TK vector (Promega) was cotransfected with reporter vector construct. Tranfections were carried out with 1 μg of total plasmid DNAs by Tfx-20 Reagent (Promega), according to the manufacturer's protocol. The DNA amount ratio of reporter and normalizing vectors for transfection was 10:1.

2.8. Reporter gene assay

Luciferase reporter gene assay (Gould and Subramani, 1988) was performed with the Dual-Luciferase Assay System (Promega) according to the manufacturer's protocol and the luciferase activity was determined by Turner Designs Luminometer, Model TD-20/20 (Promega). Six replicate measurements were performed for each reporter clone.

2.9. Gene quantitative analysis by slot blot Southern hybridization

Total genomic DNA was prepared from the livers of four individual snakes (*L. semifasciata*), as described previously (Fuse et al., 1990) and digested with *Spe*I. The plasmid DNAs containing cDNA encoding group IA PLA_2 (LsPLA2cPm09: AB037415), group IB PLA_2 (LsPLA2pkP5: AB078348) or glyceraldehyde 3-phosphate dehydrogenase (GAPDH) (LsGAPDH: AB111960) were used as the standard to calibrate the relationship between the chemiluminescent intensity and quantity of DNA molecules. The genome-digested and standard DNA samples were transferred and fixed on Hybond-N+ (Amersham Pharmacia Biotech) by aspiration under alkaline conditions with a slot blotter (Sanplatec). The blotted membranes were rinsed with 2× SSC and allowed to air dry. The sequences of the specific probes for each gene were 5′-CATCGTCAACTTTGGGTAGC-3′(for the group IA

PLA_2 gene), 5′-GCCTCCAGAACAGGTGTACG-3′ (for the group IB PLA_2 gene) and 5′-ACCCTTCATTGGGCCTTCAG-3′ (for the GAPDH gene). Labeling and detection of probe DNAs were performed with Gene Images 3′-Oligolabelling Module and ECF signal amplification module (Amersham Pharmacia Biotech), respectively, according to the manufacturer's protocol. Membranes were incubated with a detection reagent for 24 h and scanned by the FluorImager 595 (Molecular Dynamics). The images obtained were saved as TIFF files by the Image Quant ver.1.0 (Molecular Dynamics) and analyzed by KODAK 1D Image Analysis Software EDAS 292 (Eastman Kodak, version 3.5). The amounts of DNAs on the blots were determined by triplicate runs.

2.10. Quantitative real-time PCR analysis

The ABI PRISM Primer Express ver. 2.1 software (Perkin-Elmer Applied Biosystems) was used to design all PCR primers and probes (Table 2). To determine the quantity of cDNAs encoding group IA and IBPLA_2s, two sets of probes and primers were designed for each group of PLA_2 cDNA. The protein coding sequences were used to design the primers and probes. The regions used were highly conserved among the PLA_2 cDNA clones in each group.

The cDNA pools prepared from three independent snakes were used for the template of quantitative PCR. At the quantification assay for one group of PLA_2 cDNA, 0.1–10 ng cDNA pool was used for the template. The iQ Supermix (Bio-Rad) was used for the amplification of real-time PCR. TaqMan primers and probe concentrations in the final volume of 25 μl were 300 and 200 nM, respectively. The thermal cycling condition were: 3 min at 95 °C, followed by 45 cycles of 95 °C for 15 s, 60 °C for 30 s, and 72 °C 30 s. The quantitative PCR reaction was performed by iCycler iQ real-time PCR detection system (Bio-Rad). Quantity of the target cDNA in the pool were estimated from the standard curves obtained from the known amounts of target cDNA by software (ver. 3.0a) associated with the system. The quantities of the three independent reactions were averaged.

2.11. Nucleotide sequence determination

Nucleotide sequences were determined by the dideoxynucleotide chain-termination method using the ABI PRISM BigDye Terminator Cycle Sequencing Ready Reaction FS kits and ABI PRISM 377 DNA sequencer (Perkin-Elmer Applied Biosystems).

3. Results

3.1. PCR analysis of PLA_2 genes expressed in the venom glands of L. semifasciata

To investigate the expression of the group IB PLA_2 genes in the venom glands, cDNA pool from venom glands was used as a template of PCR. When loopF and #4AB primers (Fig. 1A) were used, two amplified fragments (650 and 450 bp) were detected by agarose gel electrophoresis (Fig. 1B). The size of the longer one was the same as the amplified fragment of the pancreas group IB PLA_2 cDNA clone (LsPLA2pkP5). Both fragments were cloned and sequenced (VG11: AB120375; VG8: AB120376). Both nucleotide sequences were similar to that of group IB PLA_2 clone from pancreas (Fig. 1C). Existence of two different types of genes was checked by the PCR using loopF and #4AB as primers and *L. semifasciata* genome as template (data not shown). Two types (with long or short 3′UTR) of the genes encoding PLA_2 with a pancreatic loop (group IB) exist in the genome of *L. semifasciata* and they expressed in the venom glands. The group IB PLA_2 gene, previously cloned (LsPLA2GL16-1: AB078346), had the same structure as the group IB PLA_2 mRNA with long 3′UTR.

3.2. Expression of PLA_2 genes in the venom glands of L. semifasciata

To confirm the expression of group IB PLA_2 genes in the venom glands, Northern blot hybridization analysis was performed. Before the Northern blot hybridization analysis, the specificity of the probes used for the analysis (Fig. 1A) was checked by Southern blot hybridization analysis. The probe for group IA PLA_2 weekly cross-reacted with group IB PLA_2 cDNA (Fig. 2A, middle). On the other hand, the probe for group IB PLA_2 specifically reacted with the group IB PLA_2 cDNA (Fig. 2A, bottom). As shown in Fig. 2B, group IA, the strongest signal was detected in the venom gland mRNAs with the probe for group IA in just 10 min. Because the size of the band was slightly smaller than that of pancreas mRNA, the signal detected here should be derived from group IA PLA_2 mRNA. In the case of using group IB probe, week signals were obtained when the film exposed only after 12-h exposure (Fig. 2, group IB) though no signals were obtained after 10-min and 2-h exposure (data not shown). Two bands were detected by the probe for group IB PLA_2 in the lane of venom gland mRNAs, though only one band was detected

Table 2
Primers and probes used for quantitative PCR analysis

Target	Primer 1 (5′-3′)	Reporter–5′-Probe-3′–Quencher	Primer 2 (5′-3′)
Group IA PLA_2	AATGGGATGCTACCCAAAGTT	FAM–TGGCACAGAGGGACCCTACTGCAATACA–TAMURA	CACAAGCACACACATAACGTTGA
Group IB PLA_2	GCCCCTACATCAAGATCTATTCG	FAM–ACACCTGTTCTGGAGGCAGCCTCAC–TAMURA	CCACACTCATCGTTGTCATCTC

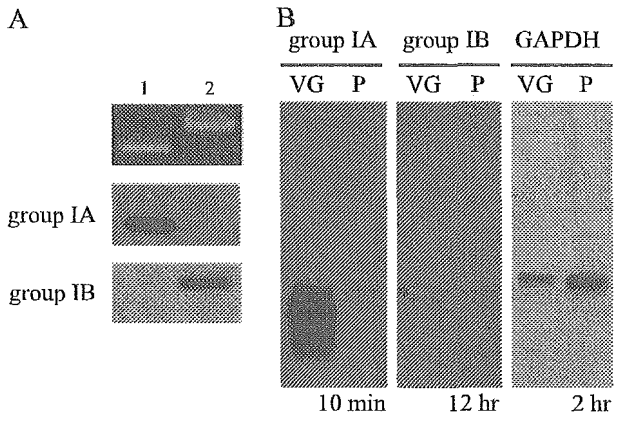

Fig. 2. Expression of PLA_2 genes in the venom glands of *L. semifasciata*. (A) Specificity of the probes was checked by Southern blot hybridization analysis. Lane 1: group IA PLA_2 cDNA (LsPLA2cPm09); lane 2: group IB PLA_2 cDNA (LsPLA2pkP5); Top panel: EtdBr staining of 100 ng cDNAs fragments; Middle and bottom panels: Southern blot hybridization analysis of 10 ng cDNA fragments. Probes were indicated in the left side of panels. The X-ray films were exposed for 1 min. (B) Northern blot hybridization analysis to the mRNAs purified from the 100 μg of total RNA of venom glands (VG) and pancreas (P). The probes using the hybridization indicated on the top of each panel. GAPDH: glyceraldehyde 3-phosphate dehydrogenase. The exposure time of the X-ray films indicated at the bottom of each panel. The asterisk mark indicates the weak signal of group IB PLA_2 with long size 3UTR in the lane of venom gland mRNA.

in the lane of pancreas mRNAs (Fig. 2, group IB). This result confirmed the presence of two types of group IB PLA_2 genes, and they expressed in the venom glands of *L. semifasciata*. These two bands probably corresponded to the cDNA clones of VG11 and VG8 (Fig. 1B). The signal intensity of the band with the longer size (Fig. 2B, asterisk) was very weak compared with the shorter one in the same lane. It suggested that the expression levels of the longer size of group IB genes were very low compared with that of the shorter size gene. The difference in the signal intensity and the exposure time required to obtain the sufficient signal suggested that the expression level of the group IB PLA_2 gene might be very low compared with those of group IA genes.

Quantitative PCR analysis also showed the substantially different amounts of mRNAs between group IA and IB PLA_2 in venom glands (Table 3). In all snakes, the amount of expressed group IA genes was around 100–300 times greater than that of group IB genes. The primers and probe for group IB PLA_2 in this assay could detect the group IB PLA_2 cDNAs regardless of the size of 3′UTR. The primers and probes for group IB PLA_2 targeted the 3′UTR could not be designed because sequence of the region did not have sufficient homology to design for all clones of group IB PLA_2 with long UTR. If such a probe were designed, the difference of expression levels would be greater than the results in Table 3. The expression levels of toxin genes in venom glands are affected with the time after the venom extraction (Lachumanan et al., 1999). The expression levels of PLA_2 genes in venom glands were slightly different among the snakes in this study, because the times after the venom extraction were not controlled on each snake.

3.3. Nucleotide sequence comparison of 5′-upstream regions of PLA_2 genes

The difference in the amount of mRNAs encoding group IA and IB PLA_2s may be caused by the regulatory elements present in the 5′-upstream region of the genes. To define the difference in the regulatory sequences, the nucleotide sequences of the 5′-upstream regions of both groups of genes, LsPLA2GL1-1 (AB062439 encoding group IA PLA_2, Fujimi et al., 2002b) and LsPLA2GL16-1 (AB078346 encoding group IB PLA_2, Fujimi et al., 2002a), were determined and analyzed. The nucleotide sequences of upstream clones (1-1up1: AB111958 and 16-1up1: AB111959) were less homologous, except for the 5′ flanking regions of the genes. As shown in Fig. 3A, even the restriction enzyme maps of the genes confirmed this observation. An inserted sequence (−444 to −34, Fig. 3B) was found in the putative promoter region of group IA PLA_2 gene. The homologous region was interrupted by this inserted sequence. The presence of the inserted sequence was probably general for the genes encoding group IA PLA_2 in *L. semifasciata*, because this sequence was also present in the another clone of group IA PLA_2 gene, which is previously isolated (LsPLA2GL5-1: AB062440) (Fujimi et al., 2002b). The promoter structure was dramatically changed by this inserted sequence in the 5′-flanking region of the group IA PLA_2 genes. In general, the minimum promoter region of a gene is present in the 5′-upstream region up to −200 from the transcription initiation site in eukaryotes. The CCAAT box, a *cis* element found in the promoter region of group IB gene (LsPLA2GL16-1), was shifted to more than 400-bp upstream in group IA gene (LsPLA2GL1-1) by the insertion of this sequence. In addition, there were one GC box and two E boxes, which were not found in the putative promoter region of group IB gene (LsPLA2GL16-1), in the 5′-upstream of group IA gene (LsPLA2GL1-1) (Fig. 3B). This observation suggested that the promoter activities

Table 3
Quantitative PCR analysis of PLA_2 genes expressed in the *L. semifasciata* venom glands

Sample	Group IA		Group IB		Ratio of average (IA/IB)
	Ave.	S.D.	Ave.	S.D.	
Snake A	3.40×10^{-7}	$\pm1.13\times10^{-8}$	1.08×10^{-9}	$\pm3.09\times10^{-10}$	315
Snake B	3.33×10^{-7}	$\pm6.71\times10^{-9}$	3.30×10^{-9}	$\pm3.86\times10^{-10}$	101
Snake C	1.47×10^{-7}	$\pm3.16\times10^{-8}$	1.51×10^{-9}	$\pm1.48\times10^{-10}$	97

The results were evaluated based on the standard curves predetermined with known amounts of target sequence. The results were derived from three independent reactions. Indicated numbers show the mole number of PLA_2 cDNA in the 1 ng venom gland cDNA pool. Ave. indicate the average of thee independent reactions. S.D. is standard deviation.

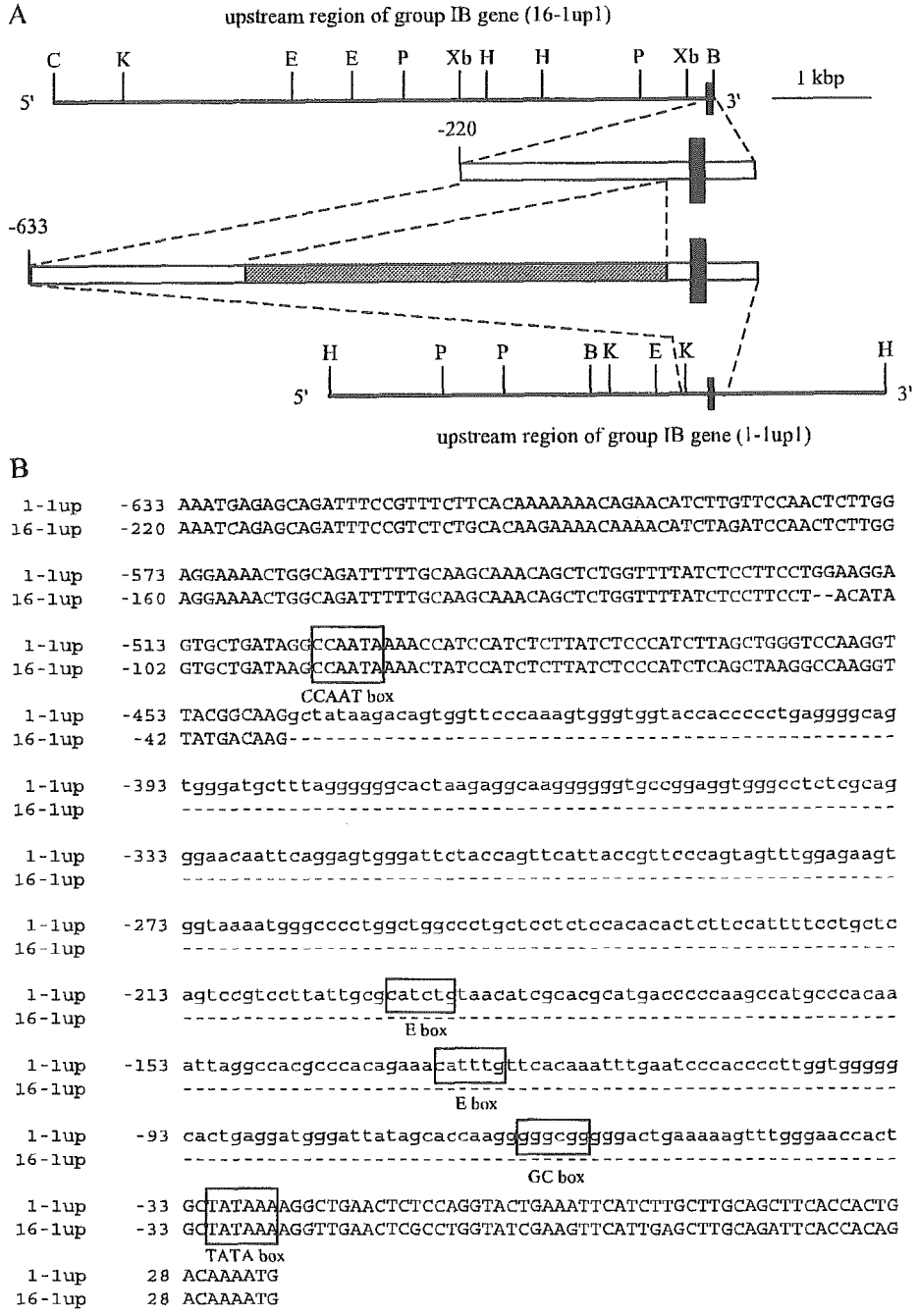

Fig. 3. Comparison of 5′-upstream region sequences of group IA and IB PLA_2 genes. (A) Restriction maps of 5′-upstream regions of group IA (1-1up1) and IB (16-1up1) PLA_2 genes are indicated. The sites of enzymes are indicated as C: *Cla*I, K: *Kpn*I, E: *Eco*RI, P: *Pst*I, Xb: *Xba*I, H: *Hin*dIII and B: *Bam*HI. Black boxes in the maps indicate exon I. Schematic representations of the homologous regions around exon I are shown between the maps. The gray region in 1-1up1 indicates the inserted sequence. (B) A nucleotide sequence comparison of 5′-flanking regions of exon I. Boxed sequences indicate the putative promoter motifs. The bar represents a gap (-). The inserted sequence is written in lowercases.

and/or tissue specific expression of these genes were/was affected by the inserted sequence in their promoter region.

3.4. Reporter gene assay

As a practicable experiment to confirm the function of the inserted sequence, reporter gene assay was performed. Ma et al. (2001) showed that the CHO cells yielded comparatively similar levels of expression to that of toxin genes in vivo and hence can be used as a cell line for the investigation of the promoter activity of toxin gene. Jeyaseelan et al. (2001) also showed that the results of reporter gene assay of a snake toxin gene using the nuclear extracts from both venom glands and CHO cells were similar.

According to their reports, we also performed the reporter gene assay with CHO-K1 cells.

A deletion series of the 5′-upstream region-luciferase gene fusion constructs was generated. The regions used for this assay were the ranges of −633 to +32 of group IA gene (LsPLA2GL1-1) and −220 to +32 of group IB gene (LsPLA2GL16-1). These regions contained both homologous and specific sequences (Fig. 3B). The transcription activity of these constructs in the CHO-K1 cell line was detected as luciferase activity (Fig. 4). Comparison of luciferase activities among the deletion series containing the 5′-upstream region of the group IA PLA_2 gene revealed that the inserted sequence significantly affected the expression ability (Fig. 4A). Two regions (−232 to −162) and (−410 to −382) especially affected the expression of group IA PLA_2 gene in CHO-K1 cell were found out in the specific inserted sequence. The former region showed the highest luciferase activity. The latter region showed the strong suppression of reporter gene transcription.

The constructs from group IA gene showed higher luciferase activity than those from group IB gene containing the corresponding regions (Fig. 4B). A construct named Δ411 was a mutant that lacked the specific inserted sequence (411 bp) from the construct IA−633. The luciferase activity of Δ411 was about one third that of IA−633 (Fig. 4B). These observations suggested that the transcription activities and/or tissue specific expression of group IA and IB PLA_2 genes were/was different from each other, and that the difference depended on the existence of a group IA PLA_2 specific inserted sequence.

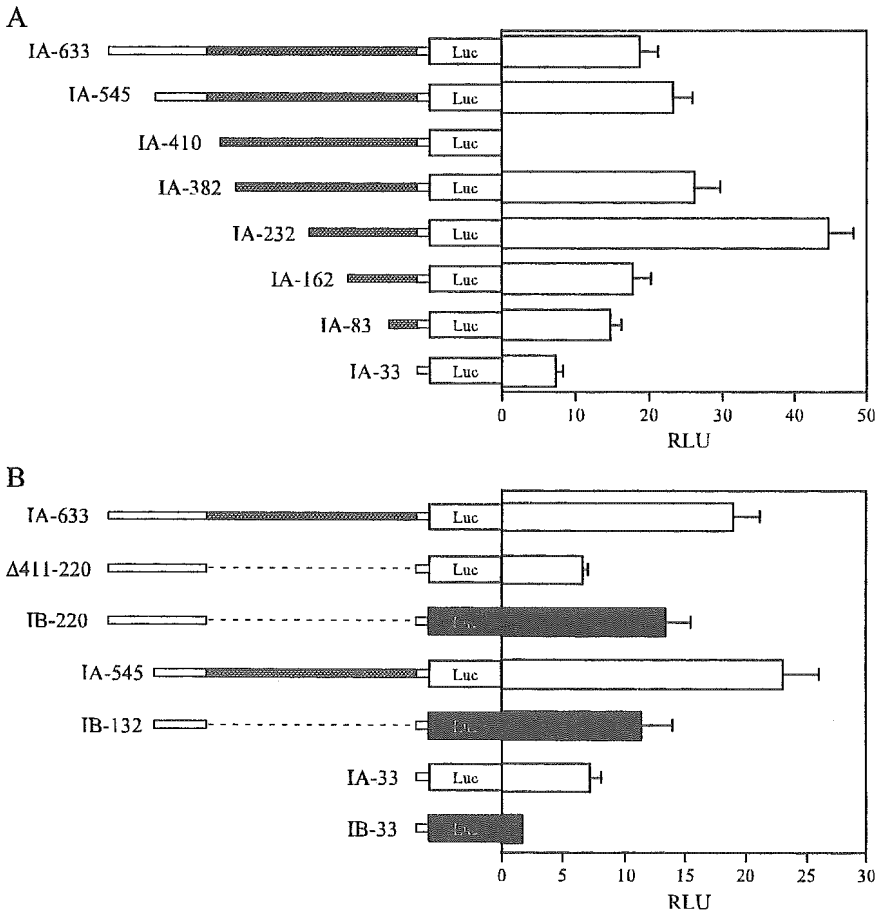

Fig. 4. Luciferase assay analysis of PLA_2 promoters. (A) Luciferase activity of the constructions from the 5′-upstream region sequence of group IA gene in CHO-K1 cell. Left: a diagrammatic representations of the 5′-upstream regions (−633 to 31) of group IA PLA_2 gene (LsPLA2GL1-1) containing the reporter gene system. Each deletion mutant was ligated to a promoter-less firefly luciferase gene (Luc) in an expression vector (pGL3B). Numbers in the names of each construction (left side of schema) indicate the distances in bp from the transcription start site. The region colored in gray is the group IA specific sequence. (B) Comparison of luciferase activities of the constructions between the derivatives from 5′-upstream regions of group IA and IB PLA_2 genes. The clones constructed from the 5′-upstream region of the group IA (LsPLA2GL1-1) gene are indicated as IA at the left side of the schema. Δ411-220 is the mutant lacking the group IA specific sequence (411 bp) from IA-633. The clones constructed from the 5′-upstream region of the group IB (LsPLA2GL16-1) gene are indicated as IB at the left side of the schema and black out the scheme of the luciferase gene. Dashed lines indicate gaps. Each activity is normalized by *Renilla* luciferase activity from a cotransfected vector (pRL-TK). RLU indicates the Relative Luciferase Unit (Firefly/*Renilla*). Data are the means of six determinations. Bar: standard deviation.

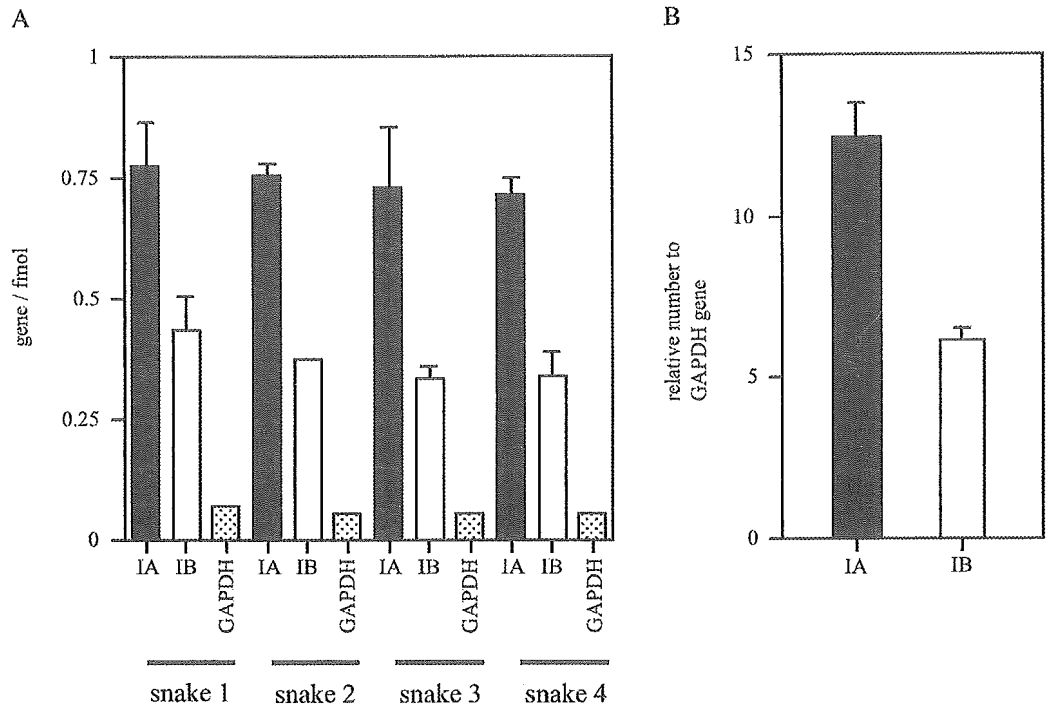

Fig. 5. Quantitative analysis of PLA_2 genes by slot blot hybridization. (A) Results for the determination of the mole numbers of three genes per 1 μg of genome DNA from four individual snakes. IA and IB correspond to the group IA and IB PLA_2 genes, respectively. GAPDH indicates the glyceraldehyde 3-phosphate dehydrogenase (GAPDH) gene. Data are the means of three determinations. Bar: standard deviation. (B) The relative numbers of each PLA_2 gene to GAPDH gene. The mole numbers of each PLA_2 gene was normalized by that of GAPDH gene. Bar: standard deviation.

3.5. Quantitative analysis of PLA_2 genes by slot blot hybridization

One of the assumable factors causing the difference in the expression level between the group IA and IB genes was their difference in the number of gene copies. To estimate the relative abundance for each PLA_2 gene (groups IA and IB) to the GAPDH gene in genomic DNA from *L. semifasciata*, quantitative analysis by slot blot hybridization was performed. From the determined chemiluminescent intensities of the fractions-blotted genomic DNA, mole number of the gene per unit mass of genomic DNA was calculated from the calibration curves. The results showed that the number of group IA PLA_2 gene copies was around 0.72–0.77 fmol/μg of genomic DNA (Fig. 5A). Using the value of the GAPDH gene as the internal standard, the abundance of each gene from four individual snakes was normalized. As a result, the abundance of the group IA PLA_2 gene was twice as much as that of the group IB PLA_2 gene (Fig. 5B). The difference in the amount of each group PLA_2 gene indicated that the contribution of the transcription mechanisms to the gene expression level in venom glands was higher than that of the gene copy numbers.

4. Discussion

In our previous paper, we described a model for the evolution of snake group I PLA_2 genes from the analysis of the structural gene sequences (Fujimi et al., 2002a). In the model, toxic PLA_2 genes arose from PLA_2 genes with a pancreatic loop coding sequence in the genome of *L. semifasciata*. However, we did not address an important question: How did the group IA genes evolve to express as toxin genes? In this report, we proposed to address this question from the analysis of the 5′-upstream regions of these genes.

Analysis of Northern blot hybridization revealed the difference of the expression level between group IA and IB genes in venom glands. In the preliminary experiment of mass spectrometry (MALDI-TOF MS) analysis, group IB PLA_2 was not detected in the venom of *L. semifasciata* (data not shown). Quantitative PCR analysis confirmed the low level of expression on group IB genes in venom glands. Expression level of group IA genes was more than 100 times higher than that of group IB genes. It seems that the group IB PLA_2 did not act as the toxin in *L. semifasciata* venom glands.

The difference of the expression level detected by the Northern blot hybridization and quantitative PCR analysis was greater than that of the copy numbers of the gene and may be explained by the difference in the transcription activity of these two genes. Analysis of the 5′-upstream sequences of group IA and IB genes from *L. semifasciata* revealed a specific inserted sequence in the 5′-flanking region of the group IA PLA_2 gene. Comparison of the 5′-flanking regions of several snake toxic group I PLA_2 genes showed that the specific inserted sequence was present before the divergence of Elapidae family (Fig. 6). It is also

```
LsGL1-1    -633 AAATGAGAGCAGATTTCCGTTTCTTCACAAAAAAACAGAACATCTTGTTCCAACTCTTGG
LsGL16-1   -220 AAATCAGAGCAGATTTCCGTCTCTGCACAAGAAAACAAAACATCTAGATCCAACTCTTGG

LsGL1-1    -573 AGGAAAACTGGCAGATTTTTGCAAGCAAACAGCTCTGGTTTTATCTCCTTCCTGGAAGGA
LsGL16-1   -160 AGGAAAACTGGCAGATTTTTGCAAGCAAACAGCTCTGGTTTTATCTCCTTCCT--ACATA

LsGL1-1    -513 GTGCTGATAGGCCAATAAAACCATCCATCTCTTATCTCCCATCTTAGCTGGGTCCAAGGT
LsGL16-1   -102 GTGCTGATAAGCCAATAAAACTATCCATCTCTTATCTCCCATCTCAGCTAAGGCCAAGGT

LsGL1-1    -453 TACGGCAAGGCTATAAGACAGTGGTTCCCAAAGTGGGTGGTACCACCCCCTGAGGGGCAG
LsGL16-1    -42 TATGACAAG----------------------------------------------------

LsGL1-1    -393 TGGGATGCTTTAGGGGGGCACTAAGAGGCAAGGGGGGTGCCGGAGGTGGGCCTCTCGCAG
LsGL16-1        ------------------------------------------------------------
PtIB       -380  CTGGTGCCTTACGGGGGCACTGAAAAGCAAGGGGGGCGCTGGAGGTGGGCCCCTCACAG
NsA        -366                              ATCTAATCCAACCACCTGCTCCAGCAGGGTTAGAA
                                             *   **        *  *     *     *   *

LsGL1-1    -333 GGAACAATTCAGGAGTGGGATTCTACCAGTTCATTACCGTTCCCAGTAGTTTGGAGAAGT
LsGL16-1        ------------------------------------------------------------
PtIB       -321 GGAACAATTCAGGGGTGGGATTCTACCGGTTCATTACCGTTCCCAGTAGTTTGGAGAACT
NsA        -331 AGGAGTGTGTGTGTGTGTGTGTGTGTGCGCACGCGCGTGCATGGTGAGTCATA-ACTT
                 * *   *    * *** *  * *    *  **    *** *   **   *   * *  *

LsGL1-1    -273 GGTAAAATGGGCCCCTGGCTGGCCCTGCTCCTCTCCACACACTCTTCCATTTTCCTGCTC
LsGL16-1        ------------------------------------------------------------
PtIB       -261 GGTAATATGGATCCCTGGCTGGCCCTGCTCCTCTCCACGCGCTCCTCCATTTTCCTGCTC
NsA        -272 AGAACACTTACTAAGCAACCGGCCATTAAGCAAGGACCACTTATATTTGGTTTGCCAGTC
                 * *   *          * **** *    *      * *     *    *** *   **

LsGL1-1    -213 AGTCCGTCCTTATTGCGCATCTGTAACATCGCACGCATGACCC-CCAAGCCATGCCCACA
LsGL16-1        ------------------------------------------------------------
PtIB       -201 ACTCAGTCCTTATTGCGCACCTGCAACATCGCACGCATGACCC-C-AA-CCACGCCCACA
NsA        -212 ACAT-GGCC-ACTTGGCCACACCCAGC--CAGTCACATGACCCACCAAGCCACGCCCATG
                *    * **   **** **     * *  *   * ******** * ** *** *****

LsGL1-1    -154 AATTAGGCCACGCCCACAGAAACATTTGTTCACAAATTTGAATCCCACCCCTTGGTGGGG
LsGL16-1        ------------------------------------------------------------
PtIB       -144 AATTAG-CCAC-CCCACAGAAACAGTTGTT-AAAAATTTGAATCCCACCCCTCCGTGGGG
NsA        -156 AATTAAGCCACGCCCACATAAACAGTTGTTAGGAAATTTGAATCCCACCCCTTGATGGGG
                ***** **** ****** ***** *****   ******************   *****

LsGL1-1     -94 G-CACTGAGGATGGGATTATAGCACCAAGGGGGCGGGGGACTGAAAAAGTTTGGGAACCA
LsGL16-1        ------------------------------------------------------------
PtIB        -87 C-CACTGAG-ATTGGATTATA-CACCAA-GGGGCGGTGGACTGAAAAA--TTTGGAACCA
NsA         -96 GGCACTGAGGATGGGATTGTAGCGCCAAGGGGGCGGTGGACTGAAGAAGTTTGGGGACCA
                  ******* ** ***** ** * **** *** *** ******** **  ** ** ****

LsGL1-1     -35 CTGCTATAAAAGGCTGAACTCTCCAGGTACTGAAA
LsGL16-1    -33 --GCTATAAAAGGTTGAACTCGCCTGGTATCGAAG
PtIB        -33 CTGCTATAAAAGGCTGAACTCACCAG-TAC-GAAA
NsA         -36 CTGCTATAAAAGGCTGAACTCGCCAGGT--GGAAATTC
                ******************** **** *    *
```

Fig. 6. Sequence comparison of the 5′-flanking regions of the group I PLA_2 genes from various snakes. The 5′-flanking regions of group IA and IB PLA_2 genes are compared. LsGL1-1 and LsGL16-1 indicate the 5′-flanking region sequences of the *L. semifasciata* group IA (AB062439) and IB (AB078346) genes, respectively. PtIB and NsA indicate the 5′-flanking region sequence of the *P. textilis* group IB PLA_2 gene (AY027495) and *N. naja sputatrix* group IA acidic PLA_2 gene (AF101235), respectively. The asterisks under the aligned sequences indicate the conserved nucleotide. The bar represents a gap (-).

significant that the functional inserted sequence in the 5′-flanking region of *L. semifasciata* group IA PLA_2 gene was also found in the *P. textilis* group IB PLA_2 gene (AY027495) expressed abundantly in venom glands. These observations indicate that the expression levels of PLA_2 genes in venom glands depend on the presence or absence of the functional inserted sequence. Ma et al. (2001) reported that the reporter gene assay of snake toxin genes in the CHO cells is proportional to the in vivo expression level. Thus, we also performed the assay using the CHO-K1 cell line. Upstream region sequences of the genes expressed in the snake venom glands were highly conserved up to around −200. The luciferase assay showed that the −232 to −162 region is important for the transcription of LsPLA2GL1-1 (group IA). Jeyaseelan et al. (2000) reported that −233 to −116 region activates the

transcription of the *Naja naja sputatrix* toxic PLA_2 (group IA) gene. The conservation of both sequences and function suggest that the mechanism of the regulation of the gene encoding toxic PLA_2 is highly conserved and under the strong selective pressure during the evolution of toxin genes.

Since group IB PLA_2s are found in many different organisms, it is appropriate to predict the presence of the sequence encoding pancreatic loop in the ancestral PLA_2 gene. We have previously presented a model for the evolution of snake toxic PLA_2 genes based on the analysis of nucleotide sequences of the structural genes (Fujimi et al., 2002a).

Following is our hypothesis related to the functional divergence of PLA_2 in snakes based the evidences in this report. During the evolution of the group IB PLA_2 genes, the functional sequence (411 bp) was inserted into the 5′-flanking region of an ancestral gene. The gene might have started to evolve as a toxin gene by gaining the expression mechanism in venom glands. To evolve as a toxic component, it is thought that a dynamic change in the transcription mechanism might have occurred before the mutation of the coding sequence. Actually, the 5′-upstream region sequences of group IA (1-1up1) and IB (16-1up1) genes were not conserved except for the 5′-flanking region of exon I (Fig. 3A). Promoter insertion is known as a dynamic alteration event of the 5′-upstream sequence associated with changes in promoter activity (Adler et al., 1988). This phenomenon occurs by the insertion of a viral sequence in the transcription regulatory region. However, such a viral sequence in the 5′-upstream regions of the genes (1-1up1 and 16-1up1) was not found by the DNA database search. Defining the origin of the functional inserted sequence found in the 5′-flanking region of *L. semifasciata* PLA_2 gene will resolve where the toxins come from.

In this study, the presence of two types of group IB genes was defined (with long or short 3′UTR). One of them, with short 3′UTR, has not been cloned yet. To define the structure of this clone will also helps us to understand the evolutionary process of snake PLA_2 genes.

Acknowledgements

This work was partially supported by grants from the Japanese Ministry of Education, Science, Sports and Culture. We gratefully acknowledge interaction with Dr. Nobuyuki Kanzawa (Biochemistry Laboratory of Sophia University).

References

Adler, H.T., Reynolds, P.J., Kelley, C.M., Sefton, B.M., 1988. Transcriptional activation of *lck* by retrovirus promoter insertion between two lymphoid-specific promoters. J. Virol. 62, 4113–4122.

Bhat, M.K., Prasad, B.N., Gowda, T.V., 1991. Purification and characterization of a neurotoxic phospholipase A_2 from Indian cobra (*Naja naja naja*) venom. Toxicon 29, 1345–1349.

Danse, J.M., Gasparini, S., Menez, A., 1997. Moleculer biology of snake venom phospholipases A_2, venom phospholipase A_2 enzymes. In: Kini, R.M. (Ed.), Structure, Function and Mechanism. Wiley, Chichester, West Sussex, pp. 29–71.

Fohlman, J., Eaker, D., Karlsoon, E., Thesleff, S., 1976. Taipoxin, an extremely potent presynaptic neurotoxin from the venom of the Australian snake taipan (*Oxyuranus s. scutellatus*). Isolation, characterization, quaternary structure and pharmacological properties. Eur. J. Biochem. 68, 457–469.

Fonteh, A.N., Samet, J.M., Surette, M., Reed, W., Chilton, F.H., 1998. Mechanisms that account for the selective release of arachidonic acid from intact cells by secretory phospholipase A_2. Biochim. Biophys. Acta 1393, 253–266.

Francis, B., Coffield, J.A., Simpson, L.L., Kaiser, I.I., 1995. Amino acid sequence of a new type of toxic phospholipase A2 from the venom of the Australian tiger snake (*Notechis scutatus scutatus*). Arch. Biochem. Biophys. 318, 481–488.

Fujimi, T.J., Kariya, Y., Tsuchiya, T., Tamiya, T., 2002. Nucleotide sequence of phospholipase A_2 gene expressed in snake pancreas reveals the molecular evolution of toxic phospholipase A_2 genes. Gene 292, 225–231.

Fujimi, T.J., Tsuchiya, T., Tamiya, T., 2002. A comparative analysis of invaded sequences from group IA phospholipase A_2 genes provides evidence about the divergence period of genes groups and snake families. Toxicon 40, 873–884.

Fuse, N., Tsuchiya, T., Nonomura, Y., Menez, A., Tamiya, T., 1990. Structure of the snake short-chain neurotoxin, erabutoxin c, precursor gene. Eur. J. Biochem. 193, 629–633.

Gao, R., Kini, R.M., Gopalakrishnakone, P., 1999. Purification, properties, and amino acid sequence of a hemoglobinuria-inducing phospholipase A_2, MiPLA-1, from *Micropechis ikaheka* venom. Arch. Biochem. Biophys. 369, 181–192.

Gould, S.J., Subramani, S., 1988. Firefly luciferase as a tool in molecular and cell biology. Anal. Biochem. 175, 5–13.

Halpert, J., Eaker, D., 1976. Isolation and amino acid sequence of a neurotoxic phospholipase A from the venom of the Australian tiger snake *Notechis scutatus scutatus*. J. Biol. Chem. 251, 7343–7347.

Jeyaseelan, K., Armugam, A., Donghui, M., Tan, N.H., 2000. Structure and phylogeny of the venom group I phospholipase A_2 gene. Mol. Biol. Evol. 17, 1010–1021.

Jeyaseelan, K., Ma, D., Armugam, A., 2001. Real-time detection of gene promoter activity: quantitation of toxin gene transcription. Nucleic Acids Res. 29, e58.

Lachumanan, R., Armugam, A., Durairaj, P., Gopalakrishnakone, P., Tan, C.H., Jeyaseelan, K., 1999. In situ hybridization and immunohistochemical analysis of the expression of cardiotoxin and neurotoxin genes in *Naja naja sputatrix*. J. Histochem. Cytochem. 47, 551–560.

Lambeau, G., Schmid-Alliana, A., Lazdunski, M., Barhanin, J., 1990. Identification and purification of a very high affinity binding protein for toxic phospholipases A_2 in skeletal muscle. J. Biol. Chem. 265, 9526–9532.

Ma, D., Armugam, A., Jeyaseelan, K., 2001. Expression of cardiotoxin-2 gene. Cloning, characterization and deletion analysis of the promoter. Eur. J. Biochem. 268, 1844–1850.

Pearson, J.A., Tyler, M.I., Retson, K.V., Howden, M.E., 1991. Studies on the subunit structure of textilotoxin, a potent presynaptic neurotoxin from the venom of the Australian common brown snake (*Pseudonaja textilis*). 2: the amino acid sequence and toxicity studies of subunit D. Biochim. Biophys. Acta 1077, 147–150.

Six, D.A., Dennis, E.A., 2000. The expanding superfamily of phospholipase A_2 enzymes: classification and characterization. Biochim. Biophys. Acta 1488, 1–19.

Tischfield, J.A., 1997. A reassessment of the low molecular weight phospholipase A_2 gene family in mammals. J. Biol. Chem. 272, 17247–17250.

Tohkin, M., Kishino, J., Ishizaki, J., Arita, H., 1993. Pancreatic-type phos-

pholipase A_2 stimulates prostaglandin synthesis in mouse osteoblastic cells (MC3T3-E1) via a specific binding site. J. Biol. Chem. 268, 2865–2871.

Yokota, Y., Ikeda, M., Higashino, K., Nakano, K., Fujii, N., Arita, H., Hanasaki, K., 2000. Enhanced tissue expression and elevated circulating level of phospholipase A_2 receptor during murine endotoxic shock. Arch. Biochem. Biophys. 379, 7–17.

Yoshida, H., Kudo, T., Shinkai, W., Tamiya, N., 1979. Phospholipase A of sea snake *Laticauda semifasciata* venom. Isolation and properties of novel forms lacking tryptophan. J. Biochem. (Tokyo) 85, 379–388.

Available online at www.sciencedirect.com
SCIENCE DIRECT®
Archives of Biochemistry and Biophysics 427 (2004) 58–67
ABB
www.elsevier.com/locate/yabbi

Biochemical and molecular biological analysis of different responses to 2,3,7,8-tetrachlorodibenzo-*p*-dioxin in chick embryo heart and liver

Nobuyuki Kanzawa,* Mariko Kondo, Tomoaki Okushima, Masatoshi Yamaguchi, Yusuke Temmei, Michiyo Honda, and Takahide Tsuchiya

Department of Chemistry, Faculty of Science and Technology, Sophia University, 7-1 Kioi, Chiyoda-ku, Tokyo 102-8554, Japan

Received 11 March 2004, and in revised form 15 April 2004

Abstract

We studied the mechanism of toxicity of 2,3,7,8-tetrachlorodibenzo-*p*-dioxin (TCDD) in the chick embryo, which is an organism highly sensitive to TCDD. TCDD was injected into egg yolks prior to embryogenesis, and eggs were incubated for 12 or 18 days. In TCDD-exposed embryos, we observed increased heart wet weight and change in the color of the liver, with abnormal fatty vesicle formation. To determine whether these effects were mediated by the aryl hydrocarbon receptor (AhR), we examined expression levels of AhR, CYP1A4, and CYP1A5. AhR was expressed continuously in the heart and liver during embryogenesis, whereas induction of CYP1A4 and CYP1A5 by TCDD was detected only in the liver. In situ hybridization study of tissue sections revealed induction of CYP1A4 in the abnormal liver tissue in which color change was not observed. To determine whether these different responses to TCDD depended on the cell type, primary cultures of chick hepatocytes and cardiac myocytes were established and 7-ethoxyresorufin-*O*-deethylase (EROD) activity was measured. Induction of EROD activity following exposure to TCDD was detected in hepatocytes but not in cardiac myocytes. Although the heart is a principal target organ for TCDD toxicity and AhR is expressed throughout embryogenesis, induction of CYP1A was not observed in the chick heart. Thus, we conclude that defects in the heart induced by exposure to TCDD occur via a different pathway than that occurring in the liver.

Keywords: AhR; Cardiac myocyte; CYP1A; Hepatocyte; TCDD

Halogenated aromatic hydrocarbons (HAHs) are ubiquitous environmental contaminants that are responsible for endocrine abnormalities in wild birds and humans. Among these chemicals, 2,3,7,8-tetrachlorodibenzo-*p*-dioxin (TCDD)[1] is the most toxic environmental contaminant. The toxic effects of TCDD can lead to wasting syndrome, carcinogenicity, teratogenicity, cardiac dysfunction, and immunodepression [1,2]. TCDD also induces abnormalities, including edema, hemorrhages, and death, in fishes [3,4], birds [5–8], and mammals [1,9]. Chicken is a highly sensitive organism and is a model to examine the effects of TCDD on developmental events [7,10,11]. Large numbers of egg-injection studies have shown that TCDD is cardiotoxic and can produce structural malformation, ventricular hypertrophy, and abnormal myocyte intracellular Ca^{2+} modulation and contractility [12–14]. Atrial natriuretic factor (ANF) is a marker for cardiac hypertrophy in adult animals [15], and increased expression of ANF has been reported in hearts of TCDD-exposed chick embryos [12]. TCDD-induced toxicities are mediated by the aryl hydrocarbon receptor (AhR) [1]. AhR is a ligand-activated transcription factor and a member of the basic helix–loop–helix/per-Arnt-Sim (bHLH/PAS) family. When a ligand such as TCDD is bound, AhR

* Corresponding author. Fax: +11-81-3-3238-3361.
E-mail address: n-kanza@sophia.ac.jp (N. Kanzawa).

[1] *Abbreviations used:* AhR, aryl hydrocarbon receptor; ANF, atrial natriuretic factor; Arnt, AhR nuclear translocator; EROD, 7-ethoxyresorufin-*O*-deethylase; GAPDH, glyceraldehyde 3-phosphate dehydrogenase; TCDD, 2,3,7,8-tetrachlorodibenzo-*p*-dioxin.

0003-9861/$ - see front matter © 2004 Elsevier Inc. All rights reserved.
doi:10.1016/j.abb.2004.04.021

translocates to the nucleus and makes a heterodimer complex with AhR nuclear translocator (Arnt). Transcriptional activation of target genes is initiated by binding of the complex to a specific region called the dioxin response element (DRE) [16,17]. The major target genes are cytochrome P450 1A1 (CYP1A1) and other CYP1A family members [18]. Two avian homologues to mammalian CYP1A1 and 1A2 that are induced by TCDD have been characterized and are designated as CYP1A4 and CYP1A5 [8,19–22]. Immunohistochemical analysis of TCDD-exposed chick embryos revealed that CYP protein was induced in various tissues, including the liver and myocardium, where AhR and Arnt co-localized [23]. Activated AhR may sequester Arnt, resulting in alteration of the Arnt-dependent pathways such as hypoxia signaling pathways and explaining the TCDD-induced abnormalities. Arnt serves as a dimer partner for a large number of transcription factors such as hypoxia-inducible factor 1a (HIF-1a) [24]. Thus, TCDD is known to mediate some teratogenic responses by binding the AhR; however, the exact induction mechanism for the cardiotoxicity is not known.

In this study, we examined the contribution of AhR expression to TCDD-induced cardiotoxicity. We found that liver was the major target of AhR-mediated TCDD toxicity in chick embryo. AhR expression was maintained at equal levels in the heart and liver during embryogenesis, but no obvious induction of CYP1A4 or CYP1A5 was detected in the heart. We conclude that TCDD affects heart and liver through different pathways during embryogenesis.

Materials and methods

Animals

White leghorn (*Gallus gallus*) fertile chicken egg (Omiya Kakin, Saitama, Japan) yolks were injected with TCDD dissolved in corn oil or with corn oil vehicle prior to incubation. Eggs were sealed with wax and incubated at 37 °C in humidified air.

TCDD exposure and morphological analysis

Eggs were injected with 1.0 pmol/g egg of TCDD (Cambridge Isotope Laboratories, Woburn, MA, USA) or vehicle (control). Control and TCDD-treated embryos were collected after appropriate incubation periods (embryonic days (E) 12 and 18). Embryos were weighed and the heart and liver were inspected. Hearts and livers then were dissected for weight and morphological analysis. Differences between treated and control embryos were analyzed by Student's t test ($P < 0.01$). For the morphological analysis, tissues were fixed overnight in 3.7% paraformaldehyde, frozen in Tissue-Tek OCT compound (Miles, Elkhart, IN, USA), and sectioned. Sections (10 μm thickness) were stained with hematoxylin and eosin and analyzed histologically.

Cell culture

Primary cultures of cardiac myocytes and hepatocytes were obtained from E12 chick embryos as described previously [13,25]. Cells were grown in Dulbecco's modified Eagle's medium (DMEM) with 10% fetal bovine serum (FBS), penicillin (100 U/ml; Sigma, St. Louis, MO, USA), and streptomycin (100 μg/ml; Meiji Seika Kaisya, Tokyo, Japan). Cells were maintained in the medium at 37 °C in a humidified atmosphere containing 5% CO_2.

EROD assay

Cells were seeded in 96-well plates at a concentration of 1×10^5 cells/well and incubated for 24 h. Thereafter, medium was removed and TCDD-containing DMEM with 5% FBS was added. Control cells were incubated in the same manner except that dimethyl sulfoxide (DMSO) instead of TCDD was added to a final concentration of 1%. After 24- or 48-h incubation, cells were washed with phosphate-buffered saline (PBS), and DMEM containing 7.4 μM ethoxyresorufin and 10 μM dicumarol with 10% FBS was added to each well. After 1 h of incubation, supernatants were transferred to new wells and the fluorescence of resorufin was measured with a Fluoroimager 595 (Amersham–Pharmacia Biotech, Little Chalfont, UK). The fluorescence intensity of each well was calculated with Kodak 1D Image Analysis Software (EDAS292, version 3.5; Eastman Kodak, Rochester, NY, USA). Intensity is given relative to control intensity with standard deviations.

Northern blot analysis

To prepare DNA probes for CYP1A4, CYP1A5, glyceraldehyde 3-phosphate dehydrogenase (GAPDH), and atrial natriuretic factor (ANF), RT-PCR was done with liver total RNA from E12 chick embryos as a template. cDNAs generated with primer pairs (summarized in Table 1) were ligated to TA-cloning vector (pGEM-T Easy, Promega, Madison, WI, USA), and the inserts were excised with *Eco*RI from isolated clones. Total RNA was isolated from heart or liver of E12 chick embryos with TriZol reagent (Gibco-BRL, Gaithersburg, MD, USA). Aliquots (20 μg) of the total RNA were electrophoresed on 1.2% formaldehyde agarose gels, and the products were transferred to nylon membranes (Hybond N^+, Amersham–Pharmacia Biotech). Samples on the membranes were hybridized according to the manufacturer's instructions (ECL Labeling and Detection System, Amersham–Pharmacia Biotech).

Table 1
Oligonucleotide primers used for PCR amplification

Gene	Accession No.[a]	Direction	Sequence
CYP1A4	X99453	Sense	5′-ATCGCCGCAATGCTTCAC-3′
		Antisense	5′-CAGACCCTTCCTTTTATTAGCC-3′
CYP1A5	X99454	Sense	5′-AGGGACCGAAGTGAACAAAG-3′
		Antisense	5′-GGTTCCGTGAGGTTATGCC-3′
GAPDH	K01458	Sense	5′-ACGCCATCACTATCTTCCAG-3′
		Antisense	5′-CAGCCTTCACTACCCTCTTG-3′
AhR	AF260832	Sense	5′-GCGCTCTTTCAAGATAAC-3′
		Antisense	5′-AGCATAACCGACTCAGAA-3′
ANF	X57702	Sense	5′-GACCCGTGCTCTGAAG-3′
		Antisense	5′-AGAGGTCCAGCATAGA-3′

[a] Accession numbers of sequences from GenBank database.

Production of anti-AhR antibody

cDNA fragment (1269 bp) was obtained by RT-PCR with primers for chicken AhR (summarized in Table 1). The fragment was ligated to pGEM-T Easy vector (Promega). The insert containing the partial coding region for AhR was obtained by digestion with *Eco*RI and further subcloned to the *Eco*RI site of the pGEX-4T-3 expression vector (Amersham–Pharmacia Biotech). The constructed vector was used for transformation of *Escherichia coli* BL21 (DE3), and recombinant AhR was purified with glutathione agarose beads according to the manufacturer's instructions (Amersham–Pharmacia Biotech). The fusion protein was digested with thrombin protease and was resolved by sodium dodecyl sulfate–polyacrylamide gel electrophoresis (SDS–PAGE) [26] followed by electrophoretic elution of AhR peptide from gels. AhR peptide was dialyzed in PBS and used as antigen. Rabbits were immunized with the antigen emulsified in Freund's complete adjuvant and boosted twice with the same antigen emulsified in Freund's incomplete adjuvant. Serum containing anti-AhR antibody was purified by incubating the serum with nitrocellulose-bound antigen and then eluting it at low pH [27].

Western blot analysis

Hearts and livers removed from chick embryos at each stage were frozen immediately in liquid nitrogen, crushed into fine powder, and dissolved in PBS containing protease inhibitors (0.2 mM phenylmethylsulfonyl fluoride (PMSF), 5 μg/ml leupeptin, and 5 μg/ml pepstatin). After centrifugation at 10,000*g* for 10 min at 4 °C, supernatants were collected, and the protein concentration was determined by the method described by Bradford [28]. Proteins (15 μg/lane) were resolved by SDS–PAGE and transferred to nitrocellulose membranes (Schleicher and Schuell, Dassel, Germany). The membranes were blocked with 5% non-fat dried milk in TPBS (0.05% Tween 20 in PBS) for 30 min at room temperature, followed by incubation with anti-AhR primary antibody overnight at 4 °C. After incubation with the primary antibody, the membranes were washed five times in TPBS and incubated for 2 h at room temperature with a 1:2000 dilution of horseradish peroxidase (HRP)-conjugated secondary antibody. Enhanced chemiluminescence (ECL) detection reagents (Amersham–Pharmacia Biotech) were used to enable detection of antibody reactivity on XAR film (Kodak).

Preparation and staining of tissue sections

Tissues were dissected, fixed with 4% paraformaldehyde in PBS overnight at 4 °C, and frozen in Tissue-Tek OCT compound (Miles). To detect lipid vesicles, sections (20 μm thickness) were washed twice with PBS for 5 min and immersed in 50% ethanol for 30 min. Visualization was achieved by immersing sections in 0.2% (w/v) Sudan IV in 70% ethanol for 1 h at 37 °C, followed by two washings with 50% ethanol for 30 s and staining with hematoxylin solution. In situ hybridization [29] was performed as previously described [30]. In brief, sections (20 μm thickness) were treated with 20 μg/ml proteinase K for 3 min at room temperature. After post-fixation with 4% paraformaldehyde in PBS for 10 min at room temperature, samples were rinsed with PBS, preincubated with the hybridization mixture for 30 min at 65 °C, and reacted overnight at 65 °C with 0.5–1 μg/ml digoxigenin (DIG)-labeled RNA probes. To obtain sense and antisense riboprobes for CYP1A4, plasmid clone prepared as described above was linearized and used as a template for the generation of riboprobes with a MAXI script in vitro transcription kit (Ambion, Austin, TX, USA). After 60 °C washes and blocking, the samples were incubated overnight at 4 °C with alkaline phosphatase-conjugated anti-DIG antibody (1:2000 dilution, Boehringer, Mannheim, Germany). After a washing to remove unbound antibodies, samples were stained with